Structure-induced diverse selective dyes adsorption and Cr(VI) photoreduction for two new polyoxometalate-based metal-viologen complexes

Xiuli Wang,*‡ Lin Yang,‡ Zhong Zhang

‡Xiuli Wang and Lin Yang contributed equally to this work and should be considered as co-first authors

College of Chemistry and Materials Engineering, Bohai University, Professional Technology Innovation Center of Liaoning Province for Conversion Materials of Solar Cell, Jinzhou 121013, P. R. China.

Corresponding Authors: Email: wangxiuli@bhu.edu.cn

Calculation of Capacity

Equation 1 was used to calculate the removal percentage of the dye.

$$R\% = [\frac{A_0 - A_t}{A_t}] \times 100 \quad (1)$$

A_0 is the absorbance of the dye solution before the adsorption process; and A_t is the absorbance of the dye solution after the adsorption process.

Table S1 Crystallographic data for **BHU-3** and **BHU-4**

Complex	**BHU-3**	**BHU-4**
Formula	$C_{72}H_{75}CuN_8O_{95}P_2W_{24}$	$C_{54}H_{55}Co_3N_6O_{57}W_{12}$
Formula weight	7110.28	4083.03
crystal system	Triclinic	Orthorhombic
space group	P_{-1}	$Pna2_1$
a/Å	13.0872(6)	14.5892(9)
b/Å	13.6972(7)	21.9646(15)
c/Å	19.4602(9)	26.1741(17)
α/°	95.4120(10)	90
β/°	106.1440(10)	90
γ/°	93.0910(10)	90
V (Å^3)	3324.2(3)	8387.4(9)
Z	1	2
D_c (g cm^{-3})	3.515	3.161
μ (mm^{-1})	20.949	17.058
F (000)	3117.0	7180.0
Reflection collected	24689	46919
Data/restraints/parameters	16325/23/900	14377/1517/1109

Goodness-of-fit on F^2	1.016	1.014
R [I>=2σ (I)]	R_1 = 0.0454, wR_2 = 0.1089	R_1 = 0.0616, wR_2 = 0.1242
R [all data]	R_1 = 0.0781, wR_2 = 0.1224	R_1 = 0.1123, wR_2 = 0.1468
$R_1 = \Sigma\|\|F_o\|-\|F_c\|\|/\Sigma\|F_o\|$, $wR_2 = \Sigma[w(F_o^2-F_c^2)^2]/\Sigma[w(F_o^2)^2]^{1/2}$		

Table S2 Partial bond distances (Å) and angles (°) for **BHU-3** and **BHU-4**

BHU-3			
Cu(1)–N(1)	2.003(11)	N(1)#1–Cu(1)–N(3)	90.6(5)
Cu(1)–N(3)	2.020(12)	N(1)#–Cu(1)–N(3)#1	89.4(5)
N(3)#1–Cu(1)–N(3)	180.0(4)	N(1)–Cu(1)–N(3)#1	90.6(5)
N(1)–Cu(1)–N(3)	89.4(5)	N(1)#1–Cu(1)–N(1)	180.0
Symmetry code: #1 2-*x*, 1-*y*, -*z*			
BHU-4			
Co(1)–O(1)	2.13(3)	N(1)–Co(1)–O(2W)	89.2(12)
Co(1)–O(2)	2.14(3)	N(3)–Co(1)–O(1)	98.2(13)
Co(1)–N(1)	2.10(2)	N(3)–Co(1)–O(2)	159.7(13)
Co(1)–N(3)	2.05(4)	N(3)–Co(1)–N(1)	104.7(12)
Co(1)–O(1W)	2.17(3)	N(3)–Co(1)–O(1W)	94.5(13)
Co(1)–O(2W)	2.17(3)	N(3)–Co(1)–O(2W)	84.3(14)
Co(2)–O(7)	2.10(3)	O(30)#1–Co(2)–O(7)	173.4(11)
Co(2)–O(30)#1	2.04(3)	O(30)#1–Co(2)–O(4W)	87.5(14)
Co(2)–N(5)	2.120(18)	O(30)#1–Co(2)–O(5W)	92.6(12)
Co(2)–O(3W)	2.04(3)	O(30)#1–Co(2)–N(5)	93.3(11)
Co(2)–O(4W)	2.12(3)	O(7)–Co(2)–O(4W)	85.9(13)
Co(2)–O(5W)	2.11(3)	O(7)–Co(2)–O(5W)	87.2(12)
O(2)–Co(1)–O(1W)	90.3(12)	O(7)–Co(2)–N(5)	93.3(11)
O(2)–Co(1)–O(2W)	90.4(12)	O(4W)–Co(2)–N(5)	179.1(14)
O(1W)–Co(1)–O(2W)	178.5(12)	O(5W)–Co(2)–O(4W)	91.8(14)

O(1)–Co(1)–O(2)	62.1(11)	O(5W)–Co(2)–N(5)	88.6(12)
O(1)–Co(1)–O(1W)	89.9(11)	O(3W)–Co(2)–O(30)#1	85.8(13)
O(1)–Co(1)–O(2W)	89.3(11)	O(3W)–Co(2)–O(7)	94.3(14)
N(1)–Co(1)–O(2)	94.8(11)	O(3W)–Co(2)–O(4W)	87.0(15)
N(1)–Co(1)–O(1W)	92.0(11)	O(3W)–Co(2)–O(5W)	178.0(14)
N(1)–Co(1)–O(1)	156.8(11)	O(3W)–Co(2)–N(5)	92.6(13)

#1 -*x*, 1-*y*, -1/2+*z*

Table S3 BVS calculations of Cu and Co atoms in **BHU-3** and **BHU-4**

BHU-3		**BHU-4**	
Cu1	1.41	Co1	1.77
		Co2	1.99
		Co3	2.50

Table S4 Selected hydrogen-bonding distance (Å) for **BHU-3** and **BHU-4**

D-H···A	D-H	H···A	D···A	D-H···A	symmetry code
BHU-3					
O1W-H1WA···O16	0.85	2.18	3.02(3)	171	*x, 1+y, z*
O2-H2···O1	0.82	2.04	2.854(19)	176	*2-x, 3-y, 1-z*
O1W-H1WB···O1	0.85	2.22	3.07(3)	172	*1-x, 2-y, 1-z*
O2W-H2WB···O48	0.85	2.09	2.930(15)	169	*1-x, 1-y, 1-z*
BHU-4					
D-H···A	D-H	H···A	D···A	D-H···A	symmetry code
O6W-H6WA···O5	0.85	1.98	2.61(5)	130	*1/2-x, 1/2+y, -1/2+z*
O6W-H6WB···O42	0.85	2.11	2.93(4)	164	*1/2+x, 1/2-y, z*

Table S5 Comparison of the adsorption rates of various adsorbents for MB

Compound	Time	Adsorption rate	Ref
$[Co(HL)(H_2O)_2(CrMo_6(OH)_6O_{18})] \cdot 5H_2O$	150 min	96.09%	[1]
$H_2[Cu_2OL_3(H_2O)_2][Ce(L)(H_2O)_3(PW_{11}O_{39})] \cdot 17H_2$	240 min	91.7%	[2]

O			
$(TBA)_3POM$-1	240 min	97.62%	[3]
$(Bpyen)_2(Mo_8O_{26})]\cdot 2H_2O$	150 min	87.3%	[4]
$\{[Cu\cdot L2'\cdot(4,4'\text{-bpy})]\cdot[Cu\cdot L2'\cdot(\beta\text{-}Mo_8O_{26})]\cdot 4H_2O\}n$	285 min	54.1%	[5]
$\{([Cu^{II}(2,2\text{-}bpy)_2]_2[PMo^{VI}{}_8V^{V}{}_2V^{IV}{}_2O_{40}(V^{IV}O)_2])[Cu^{I}(2,2'\text{-}bpy)]\}\cdot 2H_2O$	120 min	92.1%	[6]
BHU-3	120 min	97%	This work
BHU-4	1 min	97%	

Table S6 The reduction rate of **BHU-3** and **BHU-4** compared with other works

Compound	Time	Reduction rate	Ref
$\{Cu_2(OH)(Ptep)_2[H(\beta\text{-}Mo_8O_{26})]\}\cdot 2H_2O$	40 min	52.9%	[7]
$[Cu(bimeb)(H_2O)_2][(\beta\text{-}Mo_8O_{26})_{0.5}]$	40 min	54.4%	
$(H_2L_1)_2(H_2L_2)_2[Na(H_2O)]_2[Fe(H_2O)_2]\{M[P_4Mo_6O_{31}H_5]_2\}\cdot 7H_2O$	120 min	86%	[8]
$(H_2L_1)_2(H_2L_2)_2[Na(H_2O)]_2[Co(H_2O)_2]\{M[P_4Mo_6O_{31}H_5]_2\}\cdot 7H_2O$	120 min	82%	
$(H_2L_1)_2(H_2L_2)_2[Na(H_2O)]_2[Mn(H_2O)_2]\{M[P_4Mo_6O_{31}H_5]2\}\cdot 7H_2O$	120 min	76%	
$(H_2L_1)_2(H_2L_2)_2[Na(H_2O)]_2[Zn(H_2O)_2]\{M[P_4Mo_6O_{31}H_5]_2\}\cdot 7H_2O$	120 min	72%	
$[Cu_2(Cmt)_2(OH)Cl(\beta\text{-}Mo_8O_{26})_{0.5}]$	60 min	54.3%	[9]
$[Cu(H_2O)_3(H_{3/2}Tpm)_2](HTpm)(PMo_{12}O_{40})_2\cdot 4H_2O$	60 min	69.5%	
$[Cu_3Cl_2(H_2Tpm)_2(HTpm)_4(PMo_{12}O_{40})_4]\cdot 26H_2O$	60 min	56.9%	
$[Co_3(HTpm)_6(H_2O)_2(Mo_{13}O_{42})_2]\cdot 21H_2O$	60 min	66.4%	
{Ni2(DEP)2(H2O)6[H2(TeMo6O24)]}	60 min	52.3%	[10]
$\{Zn_2(DEP)_2(H_2O)_6[H_2(TeMo_6O_{24})]\}$	60 min	53.2%	
$\{Co(DEP)_2(H_2O)_2[H_2(\gamma\text{-}Mo_8O_{26})]\}\cdot 11H_2O$	60 min	54.8%	
$\{Cu(DEP)[(H_2\beta\text{-}Mo_8O_{26})_{0.5}]\}$	60 min	60.6%	
$[Cu_6(DTP)_5(OH)_2(H_2O)_6(PW^{VI}{}_{10}W^{V}{}_2O_{40})_2]$	60 min	51.7%	
$(H_2DBQ)[Fe(H_2O)_3]_2\{Fe[P_4Mo_6O_{31}H_7]_2\}\cdot 7H_2O$	120 min	91%	[11]
$(H_2DBQ)_2(H_2DBP)[Fe(H_2O)_4]\{Fe[P_4Mo_6$	120 min	86%	

$O_{31}H_7]_2\}\cdot 4H_2O$			
$(H_2DBP)_2\{Fe[P_4Mo_6O_{31}H_9]_2\}\cdot 10H_2O$	120 min	81%	
$(FPDS)_3[PW_{12}O_{40}]$	120 min	50%	[12]
$(FPDS)_4[SiMo_{12}O_{40}]$	120 min	33%	
$(FPDS)_4[SiW_{12}O_{40}]$	120 min	30%	
$(H_2bpe)_3[Zn(H_2PO_4)][Zn(bpe)(H_2O)_2]H\{Zn[P_4Mo_6O_{31}H_6]_2\}\cdot 6H_2O$	20 min	79%	[13]
$Na_6[H_2bz]_2[ZnNa_4(H_2O)_5]\{Zn[P_4Mo_6O_{31}H_3]_2\}\cdot 2H_2O$	20 min	70%	
$(H_2mbpy)\{[Zn(mbpy)(H_2O)]_2[Zn(H_2O)]_2\}\{Zn[P_4Mo_6O_{31}H_6]_2\}\cdot 10H_2O$	20 min	64%	
$(H_2bpp)_2[\{Na_4(H_2O)_5\}\{Co_{0.8}Cd_{0.2}(H_2O)_2\}\{Cd[Mo_6O_{12}(OH)_3(H_2PO_4)(HPO_4)(PO_4)_2]_2\}]\cdot 2H_2O$	180 min	74%	[14]
$(H_2bpp)_3[Zn_2\{Cd[Mo_6O_{12}(OH)_3(HPO_4)_3(PO_4)]_2\}]\cdot 6H_2O$	180 min	68%	
$[(H_2bpp)_3(bpp)_2][\{Al_2(H_2O)_4\}\{Cd[Mo_6O_{12}(OH)_3(H_2PO_4)_2(HPO_4)(PO_4)]_2\}_2]\cdot 9H_2O$	180 min	55%	
BHU-3	90 min	91.94%	This work
BHU-4	90 min	63.09%	

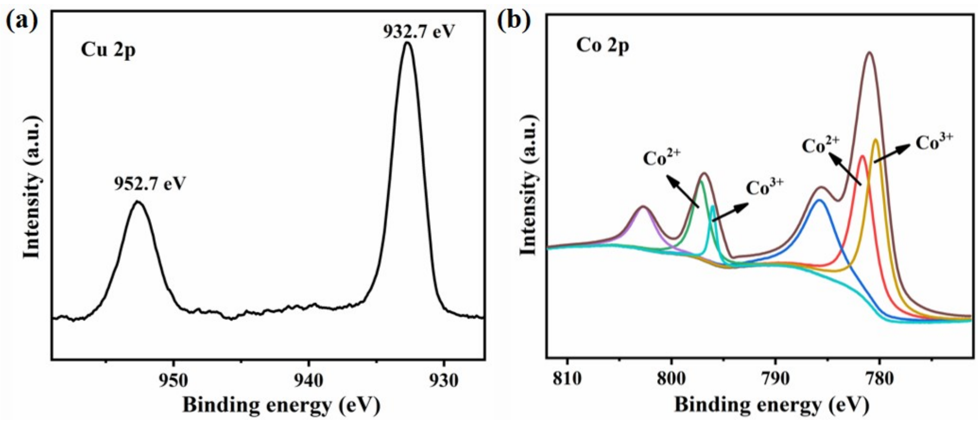

Fig. S1 The XPS spectra of Cu in **BHU-3** (a) and Co in **BHU-4** (b).

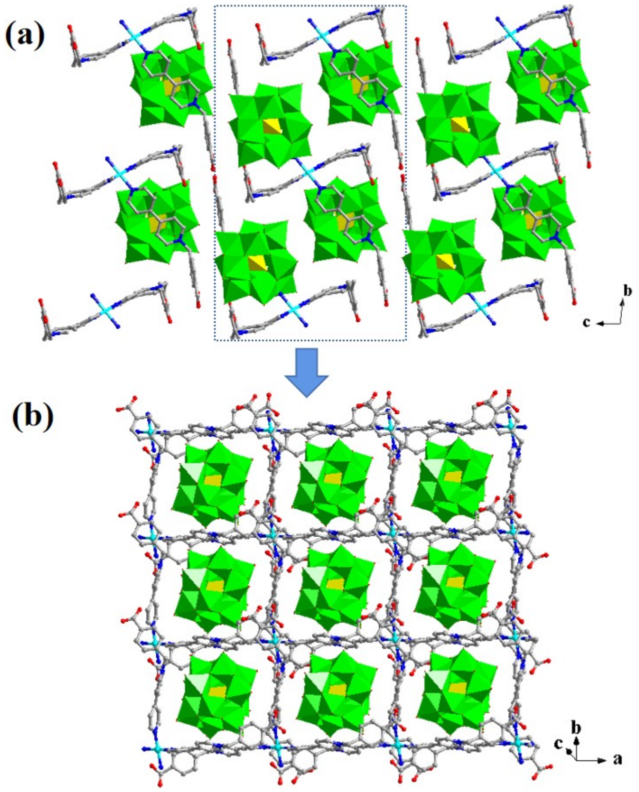

Fig. S2 The 3-D stacking of **BHU-3**.

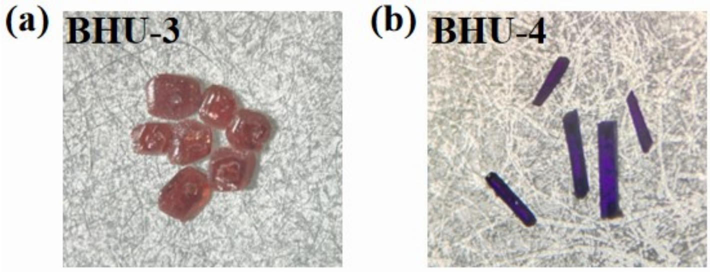

Fig. S3 The pictures of **BHU-3** and **BHU-4** under optical microscope.

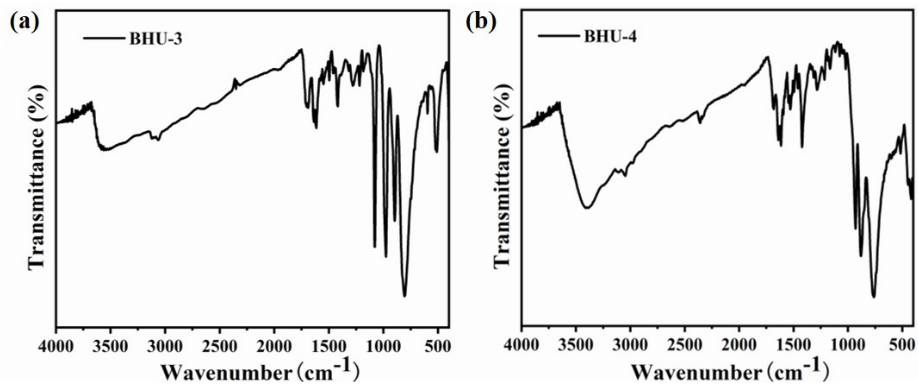

Fig. S4 The IR spectra of **BHU-3** and **BHU-4**.

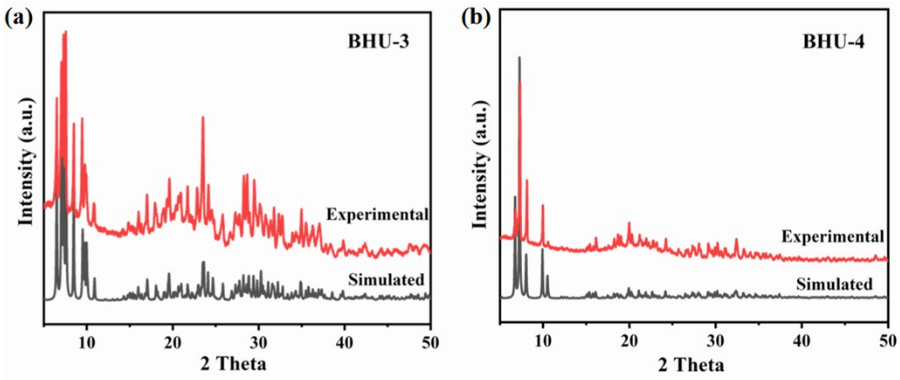

Fig. S5 The PXRD patterns of **BHU-3** and **BHU-4**.

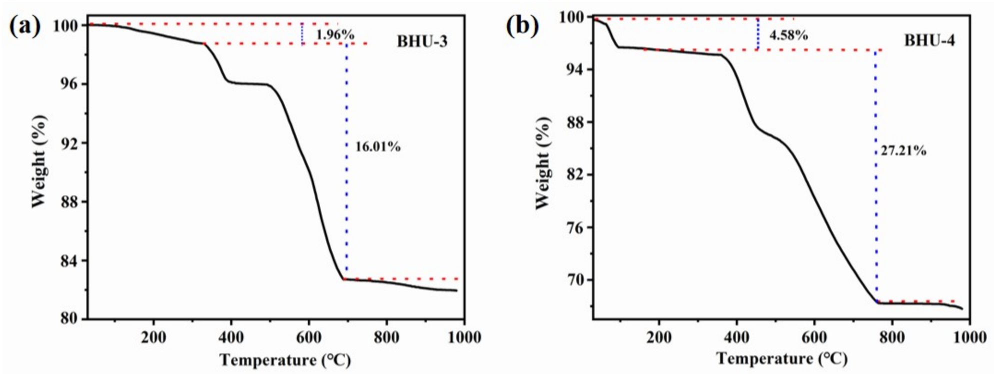

Fig. S6 The TGA curves of **BHU-3** and **BHU-4**.

The TGA curve of **BHU-3** shows that the crystal structure can be maintained before 321 °C, and the continuous weight loss between 30 and 321 °C is attributed to the removal of lattice waters (cal. 1.77% *vs.* observed 1.96%) (Fig. S5a). The TGA curve of **BHU-4** is similar to that of **BHU-3**, the crystal structure remains stable before 399 °C, and the continuous weight loss between 30 and 399 °C is attributed to the removal of lattice waters and coordination waters (cal. 4.93% vs observed 4.58%).

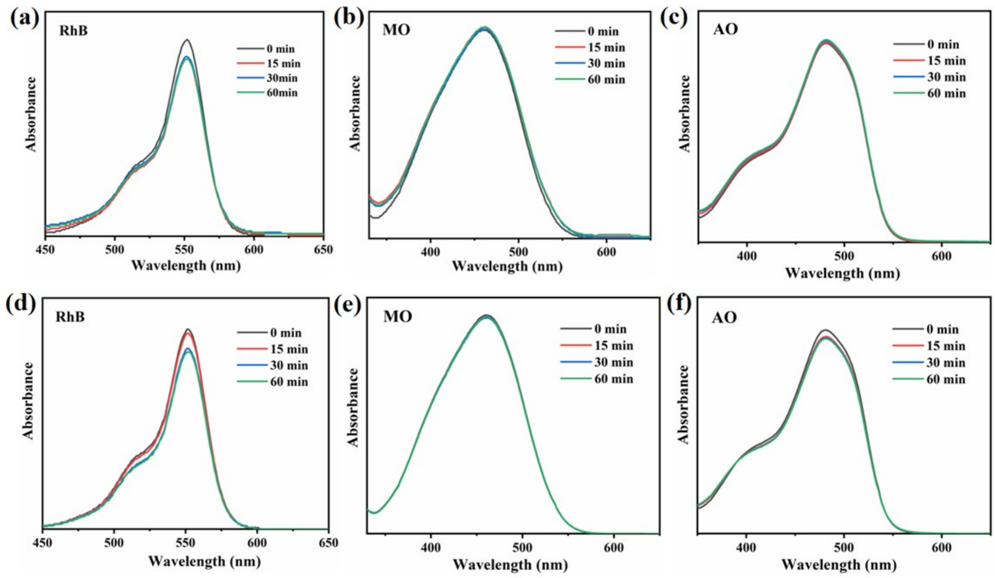

Fig. S7 The adsorption of (a-c) **BHU-3** and (d-f) **BHU-4** toward RhB, MO and AO.

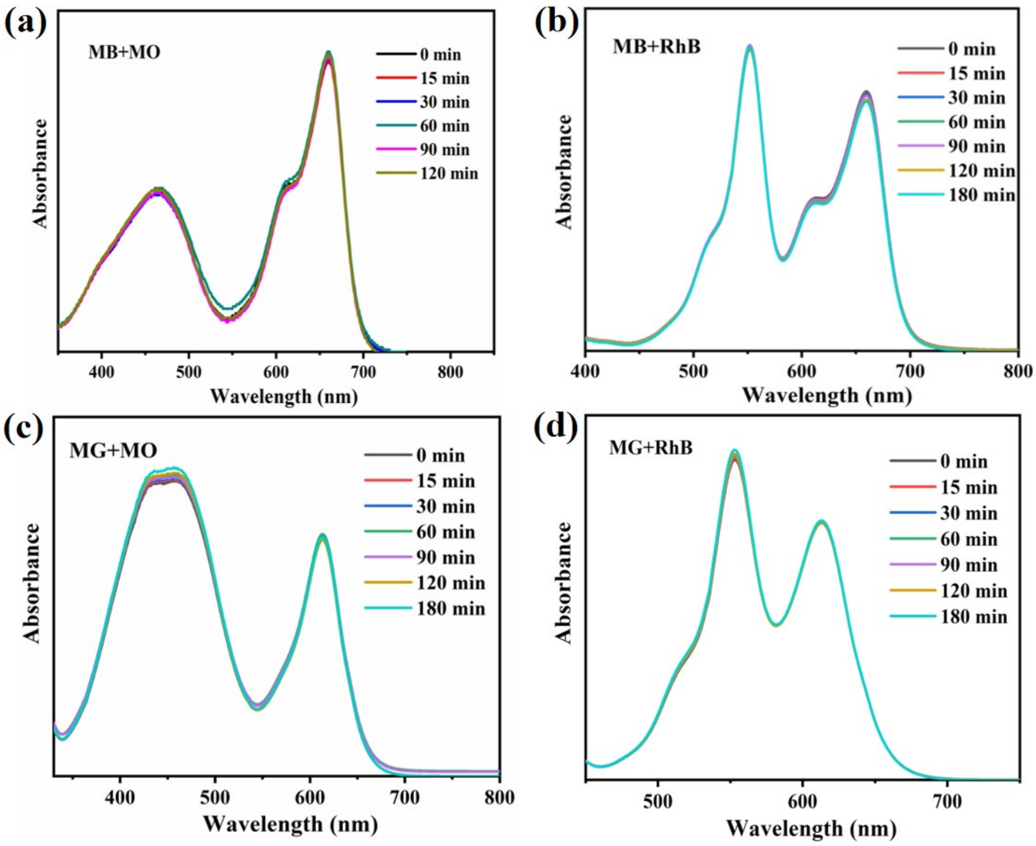

Fig. S8 The UV-vis spectra of the mixed dye solutions without catalyst.

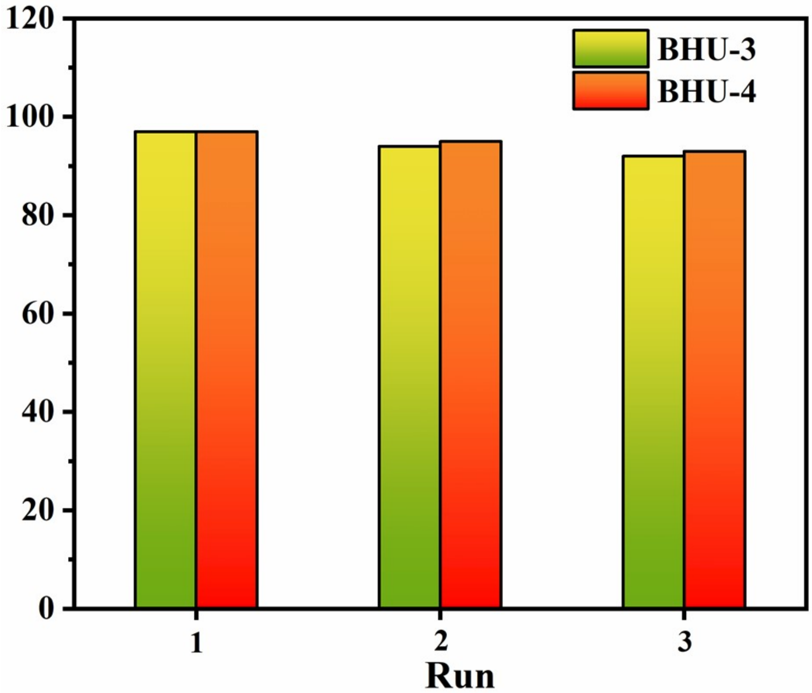

Fig. S9 The adsorption rates of **BHU-3** and **BHU-4** toward MB with 3 cycles.

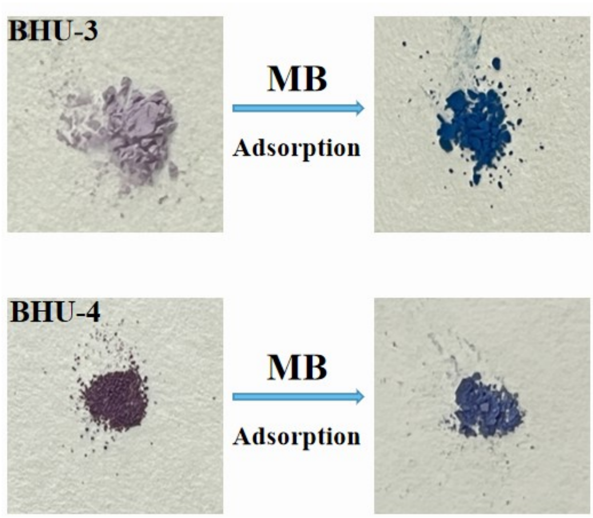

Fig. S10 The photographs of **BHU-3** and **BHU-4** before and after MB adsorption.

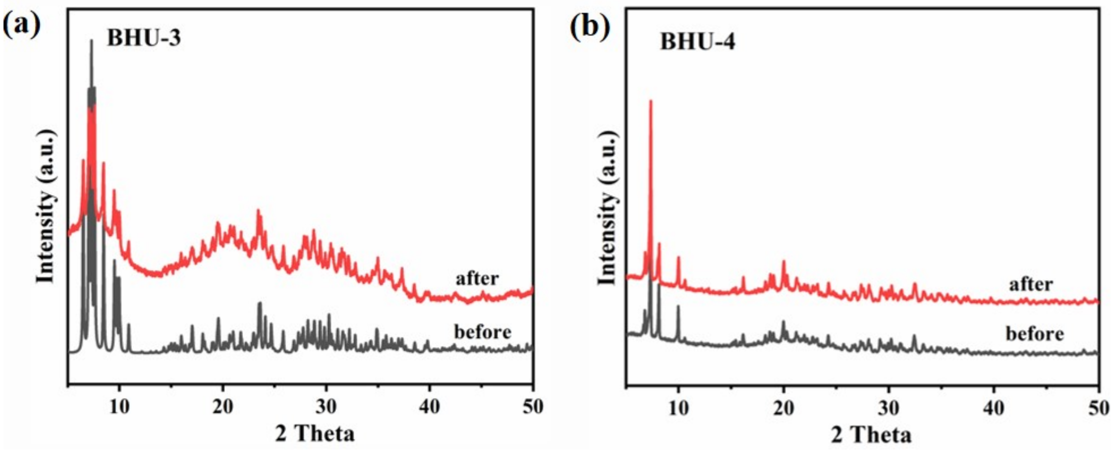

Fig. S11 The PXRD patterns of **BHU-3** and **BHU-4** toward MB adsorption before and after 3 cycles.

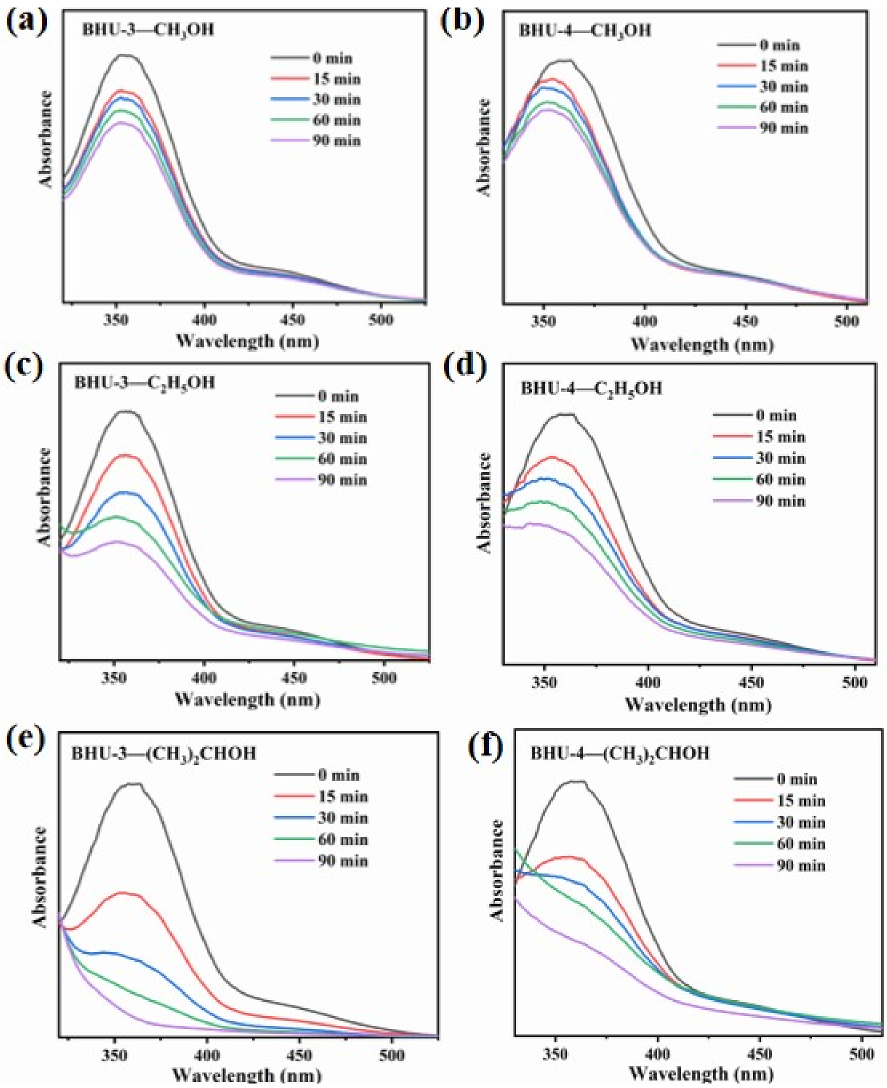

Fig. S12 Photocatalytic reduction of Cr(VI) with **BHU-3** or **BHU-4** in (a-b) methanol; (c-d) ethanol; (e-f) isopropanol.

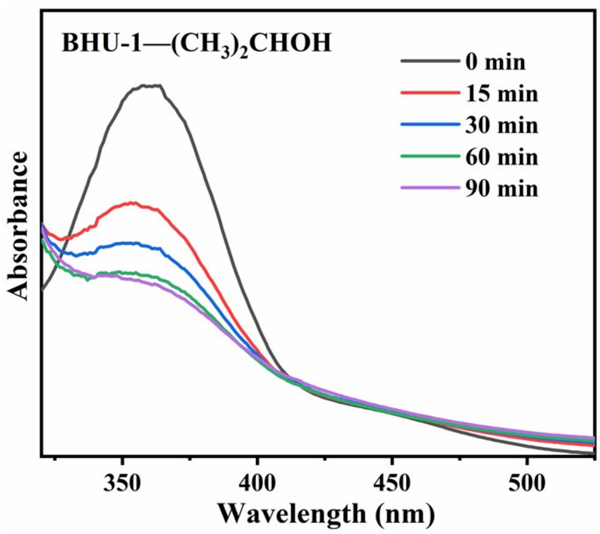

Fig. S13 Photocatalytic reduction of Cr(VI) with **BHU-1** in isopropanol.

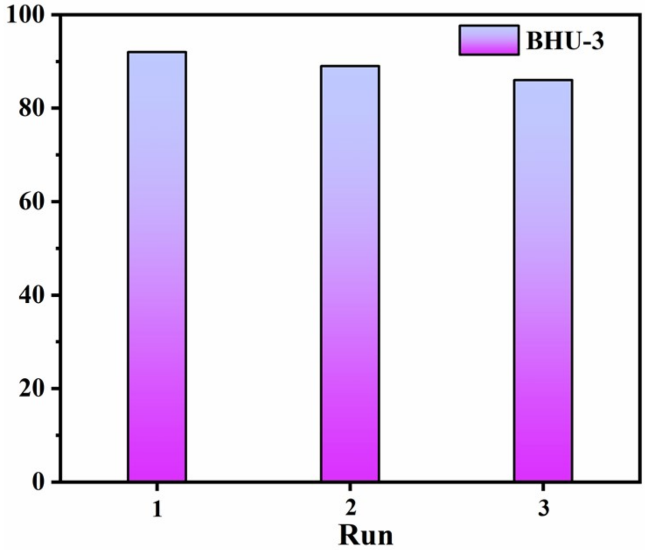

Fig. S14 The Cr(VI) photoreduction rates of **BHU-3** before and after 3 cycles.

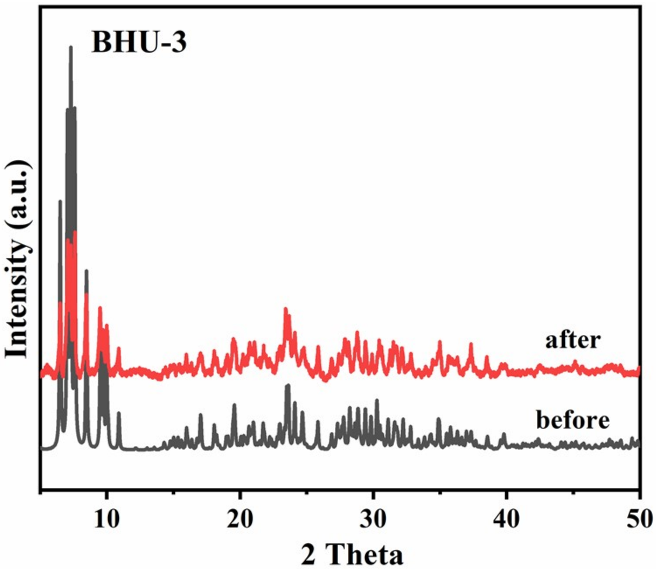

Fig. S15 The PXRD spectra of **BHU-3** toward Cr(VI) photoreduction before and after 3 cycles.

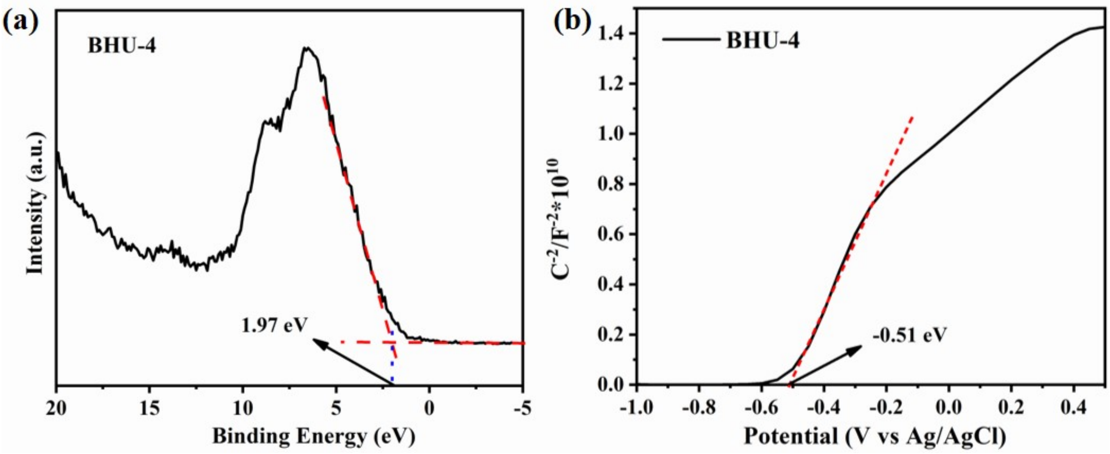

Fig. S16 The VB-XPS and MS of **BHU-4**.

References

[1] Y. Zhang, X. Wang, Y. Wang, L. Li, N. Xu and X. L. Wang, *Inorg. Chem. Front.*, 2021, **8**, 4458-4466.

[2] R. T. Zhang, H. P. Xiao, Z. Li, M. Wang, Y. F. Xie, Y. D. Ye, X. X. Li and S. T. Zheng, CrystEngComm, 2021, **23**, 2973-2981.

[3] L. Qin, Y. Pan, F.Q. Xie, L. Yu, R. R. Huai, L. Yang, D. P. Zhang, Z. Zhou, *Inorg. Chem. Commun.*, 2021, **133**, 108988.

[4] J. H. Li, X. L. Wang, G. Song, H. Y. Lin, X. Wang and G. C. Liu, *Dalton Trans.*, 2020, **49**,

1265-1275.

[5] Y. Y. Li, Y. Q. Lu, X. Y. Qiao, W. M. Huang, Y. Y. Niu, *Inorg. Chem. Commun.*, 2020, **118**, 108002.

[6] Y. B. Liu, W. T. Zhao, J. J. Zheng, H. Wang, X. B. Cui and Y. D. Chi, *Molecules*, 2023, **28**, 4706.

[7] J. Ying, C. X. Sun, L. Jin, A. X. Tian and X. L. Wang, *CrystEngComm*, 2021, **23**, 5385-5396.

[8] H. X. Bi, X. Y. Yin, X. J. Zhang, Y. Y. Ma and Z. G. Han, *CrystEngComm*, 2022, **24**, 1002-1009.

[9] S. F. Ma, J. Ying, Y. P. Zhang, A. X. Tian, CrystEngComm, 2022, **24**, 2891-2902.

[10] X. Xu, Y. P. Zhang, J. Ying, L. Jin, A. X. Tian, X. L. Wang, CrystEngComm, 2022, **24**, 1267-1278.

[11] H. X. Bi, X. Y. Yin, J. Y. He, H. Song, S. J. Lu, Y. Y. Ma, Z. G. Han, Rare Met., 2023, **42**, 3638-3650.

[12] M. Singh, A. Yadav, C. P. Pradeep, Langmuir 2022, **38**, 16034-16045.

[13] Y. Q. Zhang, L. Hou, H. X. Bi, X. X. Fang, Y. Y. Ma, Z. G. Han, chemistry-an Asian journal, 2021, **16**, 1584-1591.

[14] X. R. Tian, Y. Q. Zhang, Y. Y. Ma, Q. Zhao, Z. G. Han, Catal. Sci. Technol., 2020, **10**, 2593-2601.